Current Research in Food Science 10 (2025) 100938

Contents lists available at ScienceDirect

Current Research in Food Science

journal homepage: www.sciencedirect.com/journal/current-research-in-food-science

# Integrated metabolomics and transcriptomics analysis provides insights into biosynthesis and accumulation of flavonoids and glucosinolates in different radish varieties

Da Cai, Yanjie Dong, Lei Wang, Shancang Zhao *

*Shandong Provincial Key Laboratory of Test Technology on Food Quality and Safety, Institute of Quality Standard and Testing Technology for Agro-Products, Shandong Academy of Agricultural Sciences, Jinan, 250100, China*

ARTICLE INFO

Handling Editor: Siyun Wang

*Keywords:*
*Raphanus sativus*
Flavonoid
Glucosinolate
Metabolomics
Transcriptomics
Secondary metabolite
Radish variety

ABSTRACT

Radish is an important vegetable worldwide, with wide medicinal functions and health benefits. The quality of radish, strongly affected by phytochemicals like flavonoids and glucosinolates, are quite different depending on the radish varieties. However, the comprehensive accumulation profiles of secondary metabolites and their molecular regulatory mechanisms in different radish cultivars remain unclear thus far. Herein, we comprehensively analyzed the secondary metabolite and gene expression profiles of the flesh and skin of four popular radish varieties with different flesh and/or skin colors, using UPLC-MS/MS-based metabolomics and transcriptomics approach combined with RT-qPCR. The results showed that altogether 352 secondary metabolites were identified in radish, of which flavonoids and phenolic acids accounted for 60.51% of the total. The flesh and skin of each variety exhibited distinct metabolic profiles, making them unique in coloration, flavor, taste, and nutritional quality. The differential metabolites were mostly enriched in flavonoid biosynthesis, flavone and flavonol biosynthesis, phenylpropanoid biosynthesis, and glucosinolate biosynthesis pathway. Further, 19 key genes regulating the differential accumulation of flavonoids among different radish varieties were identified, such as *RsCHS*, *RsCCOAMT*, *RsF3H*, *RsFLS*, *RsCYP75B1*, *RsDFR*, and *RsANS* that were significantly upregulated in red-colored radish tissue. Also, 10 key genes affecting the differential accumulation of glucosinolates among different varieties were identified, such as *RsCYP83B1*, *RsSUR1*, and *RsST5a* that were significantly increased in the skin of green radish. Moreover, systematical biosynthetic pathways of flavonoids and glucosinolates and co-expression networks between genes and metabolites were constructed based on integrative analysis between metabolomics and transcriptomics. Our findings provide a novel insight into the mechanisms of radish quality formation, thereby providing a molecular basis for breeding and cultivation of radish with excellent nutritional quality.

## 1. Introduction

Radish (*Raphanus sativus* L.) belongs to the *Brassicaceae* family and is an important root vegetable crop cultivated worldwide. There are hundreds of radish landraces (Zhang et al., 2015). Radishes can be categorized according to skin and/or flesh colors, for example, white radish, green radish and red radish, which are widely cultivated and popular with consumers in China. Radishes with different flesh and/or skin colors have high variations in flavor and nutritional quality, which can be used for various purposes (Mei et al., 2022). Radish taproot has been known to contain carbohydrates, dietary fiber, vitamins, minerals, and valuable bioactive phytochemicals like flavonoids and glucosinolates (GSLs), which provide various nutrients and medicinal functions that are beneficial to human health, such as antioxidation, anti-inflammation, and anticancer activity (Zhang et al., 2020a; Barillari et al., 2005; Yi et al., 2016). The profiles and concentrations of the phytochemicals in radish taproot, which strongly affect its coloration, flavor, taste, and nutritional quality, hence directly influencing economic value and health benefits of radish, were quite differential as a result of different cultivars and growing conditions (Mei et al., 2022; Jing et al., 2012).

Flavonoids are a large class of important polyphenolic secondary metabolites, including flavones, flavonols, dihydroflavones, isoflavonoids, chalcones, flavanols, and anthocyanins (Bohm, 1998).

* Corresponding author.
*E-mail address:* shancangzhao@126.com (S. Zhao).

https://doi.org/10.1016/j.crfs.2024.100938
Received 12 August 2024; Received in revised form 11 November 2024; Accepted 25 November 2024
Available online 29 November 2024

Recently, interest in flavonoids derived from plants has greatly increased because of their vital nutraceutical properties for human. Studies have shown that the biosynthesis and accumulation of flavonoids greatly influence the color formation of plant organs and tissues (Wang et al., 2021; Zhang et al., 2020b; Li et al., 2021). Zhang et al. performed flavonoid-targeted profiling of radish, and found that red and purple radishes had anthocyanin compounds including red cyanidin, callistephin, and pelargonin (Zhang et al., 2020a). The accumulation of flavonoids is a complex process regulated by many genes and environmental factors (Zhang et al., 2018a). Several structural genes encode the enzymes necessary for flavonoid biosynthesis, such as phenylalanine ammonia lyase (PAL), cinnamate 4-hydroxylase (C4H), 4-coumarate CoA ligase (4CL), chalcone synthase (CHS), chalcone isomerase (CHI), dihydroflavonol 4-reductase (DFR), and anthocyanidin synthase (ANS) (Holton and Cornish, 1995). Zhang et al. identified candidate genes regulating anthocyanin synthesis in black radish skin, including *RsCHS*, *RsCHI*, *RsDFR*, and *RsUGT75C1* (Zhang et al., 2023). Zhang et al. found that the anthocyanin biosynthesis genes including *RsC4H*, *RsTT4*, *RsTT7*, *RsCCOAMT*, *RsDFR*, and *RsLDOX* were upregulated in red-colored and purple-colored radish accessions (Zhang et al., 2021). Liu et al. analyzed the transcriptome of 'Xinlimei' radish taproot skin, indicating that anthocyanin and chlorophyll metabolism pathways perform important roles in skin color changes (Liu et al., 2019). Muleke et al. identified 102 assembled unigenes and 20 candidate genes involved in anthocyanin biosynthesis in radish and found that total anthocyanin content correlated with transcript levels of anthocyanin biosynthesis genes, particularly *RsF3H*, *RsANS*, *RsCHS3*, *RsF3′H1*, and *RsUFGT* (Muleke et al., 2017). The above relevant reports focused primarily on anthocyanin biosynthesis genes and regulatory mechanisms. Nevertheless, there are few studies on the overall metabolic profiles and regulatory mechanisms of nonanthocyanin flavonoids. Because of the complexity and diversity of flavonoid structures as well as the complicated genetic background of radish, it is extremely necessary to integrate flavonoid metabolism phenotype with gene expression profiles to further decipher the molecular regulatory mechanisms underlying differential accumulation of flavonoids among different radish varieties, whereas the relevant research has rarely been reported thus far.

GSLs are a class of characteristic sulfur-rich secondary metabolites in Brassicaceae plants, which are classified into three major groups: aliphatic GSLs, aromatic GSLs, and indole GSLs (Halkier and Gershenzon, 2006). GSLs and their degradation products isothiocyanates have diverse bioactivities, such as defence against herbivores and resistance to pathogens in plants as well as protection of human health, especially having anti-carcinogenic properties (Razis et al., 2011; Holst and Williamson, 2004). Isothiocyanates also contribute to the flavors and tastes such as pungency (Holst and Williamson, 2004). Therefore, GSL content is one of the most important traits of radish, and crucial to nutritional quality and flavor formation of radish taproot (Holst and Williamson, 2004). Studies have reported some enzymes for GSL biosynthesis, such as branched-chain aminotransferases (BCATs), isopropyl malate isomerases (IPMIs), S-alkyl-thiohydroximate lyase (SUR1), UDP-glucosyl transferase 74 (UGT74), and sulfotransferases (SOTs) (Liu et al., 2014). Li et al. identified 13 genes that were significantly higher co-expressed in the radish genotypes with high GSL content (Li et al., 2022). Kang et al. defined the genes involved in glucoraphasatin biosynthesis process (Kang et al., 2020). However, comprehensive and detailed GSL profiles and their accumulation mechanisms in different tissues of different radish varieties are still unknown and remain to be explored.

Widely targeted metabolomics analysis, as well as more emerging technology widely targeted metabolite modificomics, combining the advantages of high resolution and wide coverage of non-target technology with high sensitivity and accurate quantitative ability of the target multiple-reaction monitoring (MRM) mode, has recently been developed and has been applied in major horticultural crops such as citrus (Wang et al., 2024), jujube (Zhang et al., 2020b), and tomato (Yang et al., 2024). As sequencing technologies advance, nowadays the combination of metabolomics with transcriptomics has become a promising approach to identify and quantify of an extremely broad range of metabolites in plants simultaneously, explore the key genes involved in metabolic pathways and corresponding regulatory mechanisms. While this approach has been applied in major crops, such as wheat (Wang et al., 2021), jujube (Li et al., 2021), and chili pepper (Heng et al., 2023), it has not yet been used in secondary metabolites of radish to our knowledge. As the characterization of global phytochemical profiles and the regulatory mechanisms in different tissues of various radish cultivars have not yet been clear so far, it is essential to investigate the comprehensive profiles of phytochemical components and their molecular regulatory mechanisms in different radish cultivars applying the integrative analysis of metabolomics and transcriptomics.

Therefore, the primary aim of this study is to comprehensively uncover the differences in secondary metabolite profiles that could contribute to the diversities of coloration, flavor, taste, and nutritional quality among different radish varieties, and further explore the underlying mechanisms regulating the differential accumulation of two important classes of secondary metabolites—flavonoids and GSLs—among different varieties. To achieve the aim, secondary metabolite profiling of the flesh and skin of four common and popular radish varieties with different flesh and/or skin colors was performed by widely targeted metabolomics analysis based on UPLC-ESI-MS/MS. Meanwhile, the global gene expression profiles were analyzed by a transcriptomics method. Moreover, we further constructed the metabolic pathways related to biosynthesis and accumulation of flavonoids and GSLs and the co-expression networks of genes and metabolites in radish taproots. These are of vital importance for in-depth and thorough understanding about the formation mechanisms of quality characteristics of different radish cultivars and helpful for improving their nutritional quality through molecular breeding.

## 2. Materials and methods

### 2.1. Plant materials

Four radish inbred lines were used in this study: Hongfeng, with red taproot skin and white flesh; White radish, with white taproot skin and white flesh; Xinlimei, with green taproot skin and red flesh; and Green radish, with green taproot skin and green flesh. All plants were grown in the experimental station of Weifang Academy of Agricultural Sciences, in August 2021. Our research complied with local guidelines and legislation, and the required permissions and licenses for the study were obtained. Developed taproots were harvested at the end of October 2021. The skin and flesh of the taproots were separated using a blade on a clean table, sampled, and stored at −80 °C for further analysis. Each sample included three biological repeats and each repeat included five individual plants.

### 2.2. Determination of moisture content, antioxidant capacity, total polyphenols, and total flavonoids

The moisture content of fresh radish was determined according to GB 5009.3 (National Standards of China GB 5009.3-2016, 2016). The antioxidant capacity of radish was analyzed by the ABTS method with the total antioxidant capacity assay kit (Beyotime, Shanghai, China). The results of antioxidant capacity were expressed as the Trolox-equivalent antioxidant capacity. The total polyphenols were analyzed by the Folin-Ciocalteu method according to GB/T 8313 (National Standards of China GB/T 8313-2018, 2018), and the concentration was calculated from a calibration curve using gallic acid (Alta Scientific Co., Ltd., Tianjin, China) as the standard. The total flavonoids were determined according to NY/T 1295 (Agricultural Industry Standard of China NY/T 1295-2007, 2007), and the content was calculated from a calibration curve using rutin (Alta Scientific Co., Ltd., Tianjin,

China) as the standard. Concentrations of total polyphenols and total flavonoids were expressed as gram per 100 g on a dry-weight basis.

### 2.3. Metabolomics analysis

The samples were prepared based on the method described by Zhu et al. (2018). In detail, the samples were freeze-dried and then were crushed. The 50 mg of lyophilized powder was dissolved with 1.2 mL of 70% methanol solution, and vortexed for 30 s every 30 min for 6 times in total. Following centrifugation at 12000 rpm for 3 min, the extracts were filtrated through a microfilter (0.22 μm pore size) before UPLC-MS/MS analysis. Equal amounts of each sample were mixed to prepare the quality control (QC) sample to ensure the reliability of the analytical method and data. The QC sample was inserted before, during, and after sample analysis.

The sample extracts were analyzed using an UPLC-ESI-MS/MS system (UPLC, SHIMADZU Nexera X2; MS, Applied Biosystems 4500 Q TRAP). Chromatographic separations were performed with an Agilent SB-C18 (1.8 μm, 2.1 mm × 100 mm). The mobile phase consisted of pure water with 0.1% formic acid (A) and acetonitrile with 0.1% formic acid (B) with the following gradient elution: 0 min, 95% A and 5% B; 0–9 min, 5% A and 95% B; 9–10 min, 5% A and 95% B; 10–11.1 min, 95% A and 5% B; and 11.1–14 min, 95% A and 5% B. The flow velocity was set to 0.35 mL/min. The column oven was maintained at 40 °C. The injection volume was 4 μL. Peak detection was performed by an ESI-triple quadrupole-linear ion trap (Q TRAP) mass spectrometer.

The mass spectrometry parameters were as follows: source temperature of 550 °C; ion spray voltage (IS) of 5500 V (positive ion mode)/-4500 V (negative ion mode); ion source gas I, gas II, and curtain gas were set at 50, 60, and 25 psi, respectively; the collision-activated dissociation was high. QQQ scans were acquired as MRM experiments with collision gas (nitrogen) set to medium. DP and CE for individual MRM transitions were done with further DP and CE optimization. A specific set of MRM transitions were monitored for each period according to the metabolites eluted within this period.

### 2.4. Transcriptome analysis

Total RNA of each sample was extracted using the Tiangen RNAprep Pure kit for plants (Tiangen, Beijing, China), and examined with a NanoPhotometer spectrophotometer (IMPLEN, CA, USA), Qubit 2.0 Fluorometer (Life Technologies, CA, USA), and a Bioanalyzer 2100 system (Agilent, CA, USA). Transcriptome sequencing was performed by Metware Biotechnology Co. Ltd. (Wuhan, China). RNA-seq libraries were constructed. The library preparations were sequenced on an Illumina platform and 150 bp paired-end reads were generated. After quality control and filtration, the clean reads were mapped to the reference genome GCF_000801105.1 (https://www.ncbi.nlm.nih.gov) using HISAT v2.1.0 (Kim et al., 2015).

### 2.5. Validation of gene expression

To validate the reliability of the RNA-seq data, the relative transcript levels of 12 genes were analyzed by RT-qPCR with specific primers (Supplementary Table S1). The cDNA synthesis and RT-qPCR were performed as previously described (Zhang et al., 2018b). The first-strand cDNA was synthesized with the All-in-One RT Mixture IV (ABM, Canada). The cDNA template was subjected to qPCR using the SYBR Green Real time PCR Master Mix (DBI, Germany). *Actin* was used as an internal control for the normalization of gene expression. The relative expression levels were calculated using the delta CT method (Schmittgen and Livak, 2008). Three independent biological replicates with three technical replicates each were analyzed by RT-qPCR to ensure reproducibility and reliability.

### 2.6. Data processing and statistical analysis

The signal intensities of metabolites obtained by UPLC-MS/MS were scaled before multivariate statistical analysis. Unsupervised principal component analysis (PCA) was carried out by statistics function prcomp in R (www.r-project.org). The hierarchical cluster analysis (HCA) and supervised orthogonal projections to latent structures discriminant analysis (OPLS-DA) were performed by R package ComplexHeatmap and MetaboAnalystR, respectively. The data were log-transformed and mean-centered before OPLS-DA. A permutation test (200 permutations) was carried out in order to avoid overfitting. The metabolites with VIP $\geq$1 and $|\log_2$ fold change$| \geq 1$ were identified as the significant differential metabolites. The metabolomics pathway analysis was performed using the KEGG database.

The quantification of the gene expression level applied StringTie v1.3.4 d to calculate FPKMs (Fragments per kilo-base of exon per million fragments mapped). DESeq2 v1.22.1 was used to identify differentially expressed genes (DEGs), and the $p$ value was corrected using the Benjamini-Hochberg method to obtain the false discovery rate (FDR). Transcripts with FDR $<0.05$ and $|\log_2$ fold change$| \geq 1$ were identified as DEGs. The KEGG enrichment analysis is performed based on the hypergeometric test.

The correlation analysis between gene expression and metabolites was carried out by R. The Pearson correlation coefficients between the expression levels of DEGs and the contents of metabolites were calculated. Then the correlation network was constructed by Cytoscape 3.8.2. The statistical significance was set at $p < 0.05$.

## 3. Results

### 3.1. Morphology and conventional physicochemical and nutritional indicators of radish taproots

The four radish accessions were planted and grown under uniform conditions in the same season. The morphology of the radish taproots, particularly the color of skin and flesh, were obviously different. White radish has white taproot skin (WS) and white flesh (WF), Green radish has green taproot skin (GS) and green flesh (GF), Xinlimei radish has green taproot skin (XLMS) and red flesh (XLMF), and Hongfeng radish has red taproot skin (RSWFS) and white flesh (RSWFF) (Fig. 1A).

The moisture content, antioxidant capacity, and contents of total polyphenols and total flavonoids of skin and flesh of four radish varieties were first analyzed. As shown in Fig. S1, the moisture content of different radish samples was in the range of 87.7%–94.6%. The antioxidant capacity was highest in red-colored radish tissue XLMF (1.19 mmol/kg) and RSWFS (1.05 mmol/kg) ($p < 0.05$), followed by GS and GF (Fig. 1B and C). Numerous studies reported that polyphenols were responsible for the antioxidant ability in agricultural products, and flavonoid was the most important polyphenol in radish. As shown in Fig. 1B and C, the total polyphenols and flavonoids in skin and flesh of four different varieties ranged in 0.3–1.9 and 0.1–0.6 g/100 g dw, respectively. Noteworthily, the total polyphenols and flavonoids were highest in XLMF (total polyphenols: 1.9 g/100 g; total flavonoids: 0.6 g/100 g) ($p < 0.05$), followed by RSWFS (total polyphenols: 1.3 g/100 g; total flavonoids: 0.5 g/100 g) ($p < 0.05$), while in RSWFF, they were relatively low and only 0.3 and 0.1 g/100 g, respectively. Therefore, it can be concluded that there must be huge discrepancies in metabolites among different radish varieties and different tissue. Thus, the small-molecule metabolites in skin and flesh of four radish varieties were analyzed in the next study.

### 3.2. Comprehensive profiling of secondary metabolites in the flesh and skin of different radish varieties

A widely targeted metabolomics analysis based on UPLC-MS/MS was performed for comprehensive profiling of secondary metabolites in

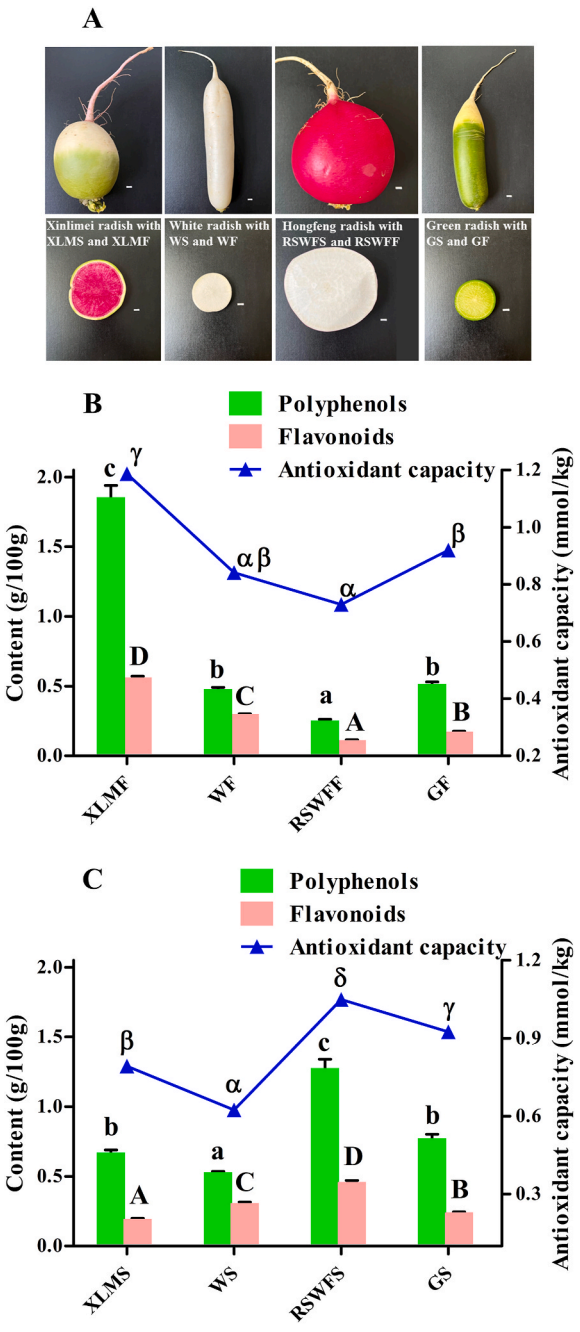


**Fig. 1.** Different skin and flesh color phenotypes of radish (A), contents of total polyphenols and total flavonoids and antioxidant capacity of flesh and skin of four radish varieties (B, C). (A) Scale bar = 1 cm. (B) and (C) Concentrations of total polyphenols and total flavonoids were expressed as g/100 g dw. Antioxidant capacity was expressed as the Trolox-equivalent antioxidant capacity with the unit mmol/kg. Values without a common letter within the same indicator were significantly different, $p < 0.05$. The significant differences among different groups were analyzed by LSD test. Abbreviations: XLMF, Xinlimei radish taproot flesh; XLMS, Xinlimei radish taproot skin; WF, White radish taproot flesh; WS, White radish taproot skin; RSWFF, Hongfeng radish taproot flesh; RSWFS, Hongfeng radish taproot skin; GF, Green radish taproot flesh; GS, Green radish taproot skin.

radish taproots. A total of 352 secondary metabolites were identified (Supplementary Table S2), including 118 flavonoids, 95 phenolic acids, 67 alkaloids, 28 GSLs, 12 lignans, 11 coumarins, 8 terpenoids, and 13 other compounds, which are the important foundation of radish nutritional quality. Polyphenolic components, including flavonoids and phenolic acids, accounted for 60.51% of the identified compounds, indicating that polyphenols in radish were dominant bioactive constituents.

To understand differences in global metabolic profiles among different radish varieties, unsupervised PCA was performed to assess the overall secondary metabolite differences in the flesh and skin among four radish cultivars. As shown in Fig. 2A, the PCA scores plot depicted a clear separation among the flesh and skin samples of four radish cultivars, implying that the phytochemicals in radishes with different skin and flesh colors were distinct and there were also significant nutritional discrepancies between radish flesh and skin. Also, the QC samples were tightly clustered, indicating high repeatability of the metabolomics data in the analysis process. The total ion chromatography (TIC) overlap diagrams at $ESI^+$ and $ESI^-$ modes of QC samples also revealed the reliability of the data (Fig. S2). Sample-to-sample correlation analysis showed that the correlation was greater than 0.9 between each repeat of radish samples, indicating that the repeatability was desirable among biological replicates of radish samples, and the data obtained in this study were reliable (Fig. S3). Additionally, HCA combined with a heat map was carried out to directly reflect the differences in the accumulation patterns of secondary metabolites among different groups (Fig. 2B). Secondary metabolites could be grouped into seven clusters. In detail, the metabolites in clusters 4 prominently accumulated in GS, and primarily involved GSLs like 4-methylthiobutyl GSL, benzyl GSL, and 7-(methylsulfinyl) heptyl GSL. The metabolites in clusters 5 were primarily represented by flavonoids and phenolic acids such as rutin, caffeic acid, and anthocyanin, and these highly accumulated in RSWFS. The metabolites in clusters 6 commonly distributed in XLMF and RSWFS, and were primarily composed of antioxidant components including flavonoids, phenolic acids, GSLs, and alkaloids. These results essentially coincided with the above data on total flavonoids, total polyphenols, and antioxidant capacity. The metabolites in clusters 7 highly accumulated in WS and WF. The metabolites in clusters 2 prominently distributed in GF and RSWFF. The metabolites involved in clusters 1 commonly accumulated in XLMS. Thus, the results of HCA indicated that the skin and flesh samples of these four radish accessions had distinct metabolite profiles, which were consistent with the results of PCA analysis.

To determine the metabolites that caused the observed differences, a pairwise comparison of the four radish accessions was conducted by OPLS-DA. There are a clear separation between XLMF and WF, XLMF and GF, XLMF and RSWFF, GF and WF, RSWFF and WF, GF and RSWFF, XLMS and WS, GS and WS, RSWFS and WS, RSWFS and GS, XLMS and GS, and RSWFS and XLMS in the OPLS-DA scores plots (Figs. S4 and S5), further indicating that there are distinct differences in the global metabolic profiles between the different groups. The two criteria VIP $\geq$1 and $|\log_2$ fold change$| \geq 1$ were applied to identify the differential metabolites. The results are presented as volcano plots (Fig. 2C–2H, Fig. S6). It is worth noting that there were 153 (101 upregulated and 52 downregulated), 138 (102 upregulated and 36 downregulated), and 154 (113 upregulated and 41 downregulated) differential metabolites for XLMF, compared to WF, GF, and RSWFF, respectively (Fig. 2C–2E). These results mean that the quantities of upregulated compounds were far more than that of the downregulated components for XLMF compared to the flesh of the other three radish accessions, indicating that the majority of secondary metabolites were much more abundant in XLMF and XLMF was a rich source of phytochemicals. The upregulated phytochemicals included 66 (39 flavonoids and 27 phenolic acids), 63 (34 flavonoids and 29 phenolic acids), and 67 (35 flavonoids and 32 phenolic acids) polyphenolic components in XLMF, compared to WF, GF, and RSWFF, respectively, accounting for 65%, 62%, and 59% of the upregulated compounds respectively, which suggested that polyphenols, particularly flavonoids, were important metabolites greatly contributing to the distinct quality discrepancies among different radish varieties. Additionally, it should be noted that there were 160 (112 upregulated and 48 downregulated), 172 (118 upregulated and 54 downregulated), and 172 (111 upregulated and 61 downregulated)

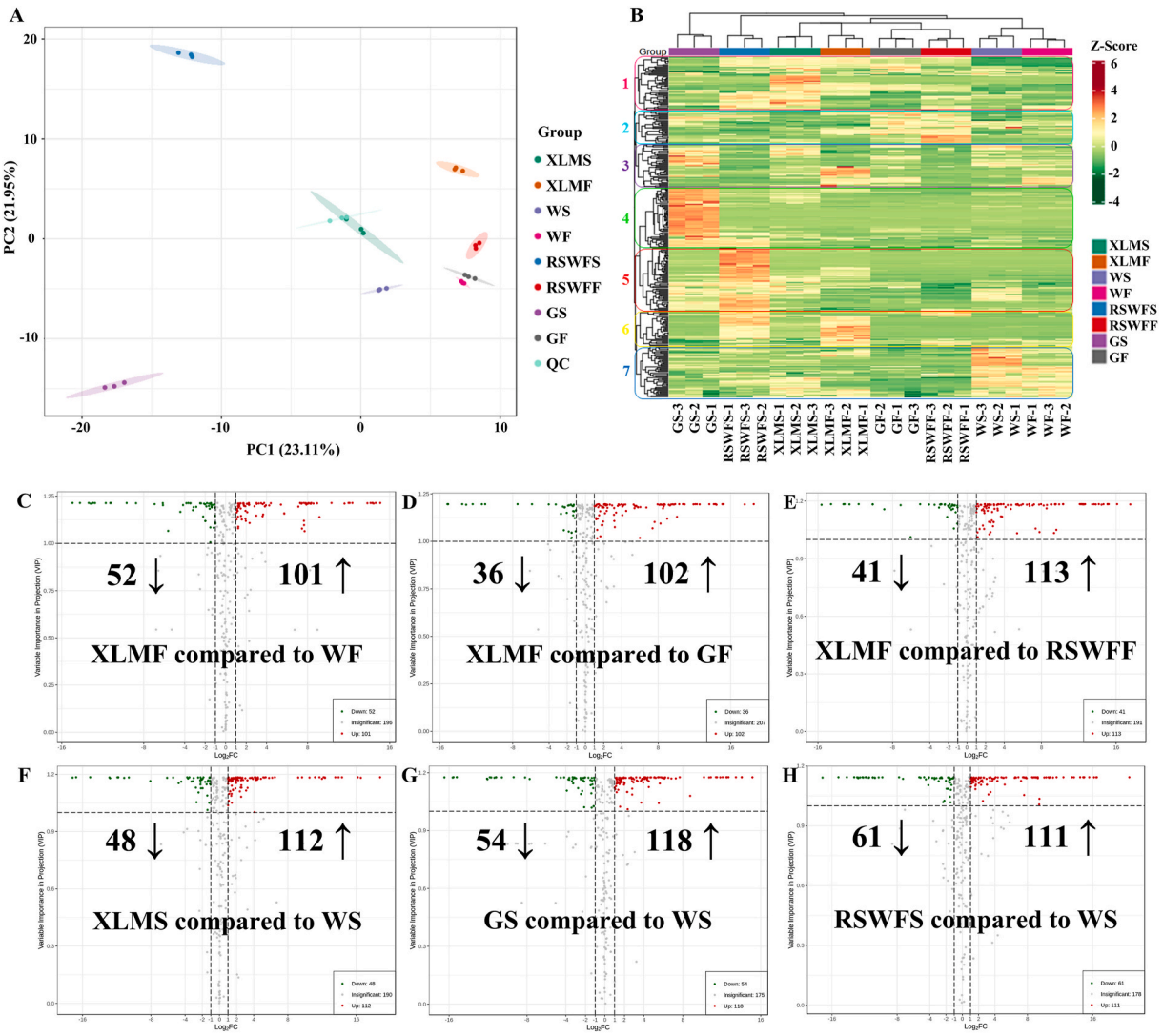


**Fig. 2.** Differences of secondary metabolites in the flesh and skin of different radish cultivars. (A) Score plot of PCA of secondary metabolites reflects high cohesion within groups and a clear separation among different groups. (B) Heat map visualization of HCA of secondary metabolites. Each metabolite is visualized in one row, and each sample is represented by one column. Progressive colors show the relative accumulation levels of metabolites from low (green) to high (red). (C)~(H) OPLS-DA volcano plots of XLMF compared to WF (C), XLMF compared to GF (D), XLMF compared to RSWFF (E), XLMS compared to WS (F), GS compared to WS (G), and RSWFS compared to WS (H). Volcano plots reveal the identified differential metabolites between the two groups. Green spots represent downregulated differential metabolites, red spots represent upregulated differential metabolites, and gray spots denote detected metabolites with insignificant differences.

differential metabolites for XLMS, GS, and RSWFS, respectively, compared to WS (Fig. 2F–2H). These results reflected that the amounts of upregulated components were far more than that of the down-regulated compounds for XLMS, GS, and RSWFS compared to WS, implying that most secondary metabolites were much more abundant in colored skin.

To obtain detailed pathway information, the differential metabolites were mapped to the KEGG database and enrichment analysis was performed (Figs. S7 and S8). The differential metabolites were mostly enriched in flavonoid biosynthesis, flavone and flavonol biosynthesis, phenylpropanoid biosynthesis, phenylalanine metabolism, GSL biosynthesis and 2-oxocarboxylic acid metabolism. Therefore, these metabolic pathways should be key pathways responsible for the polymorphisms of coloration, flavor, and nutritional quality among different radish varieties. Thus, an in-depth analysis on these metabolic pathways relevant to flavonoid and GSL biosynthesis in different radish cultivars was carried out in the next study.

### *3.3. Transcriptomic profiling of the flesh and skin of different radish varieties*

To elucidate the differences in transcription levels among the different radish varieties, RNA-seq analysis of the flesh and skin of the four radish accessions was performed, generating a total of 1,141,515,178 raw reads (Supplementary Table S3). Raw reads were uploaded to NCBI (SRA accession no. PRJNA1180643). After adaptor sequence trimming and filtering out of low-quality reads, a total of 1,109,142,030 clean reads and 166.35 G clean bases were obtained. The Q20 percentages ranged from 96.32% to 96.93%, and the GC percentages ranged from 45.20% to 47.23%. Of these clean reads, 81.43%–86.05% were mapped to the radish reference genome. Among these, 73.86%–78.32% were mapped uniquely to one location. Therefore, the results showed that the data were reliable and sufficient.

The DEGs were identified by pairwise comparisons of the expression levels between the four radish accessions, based on the two criteria $|\log_2$ fold change$| \geq 1$ and FDR $<0.05$, as shown in Fig. 3A. As to radish flesh, there were 14998, 11139, 13971, 15159, 13838, and 12985 DEGs for

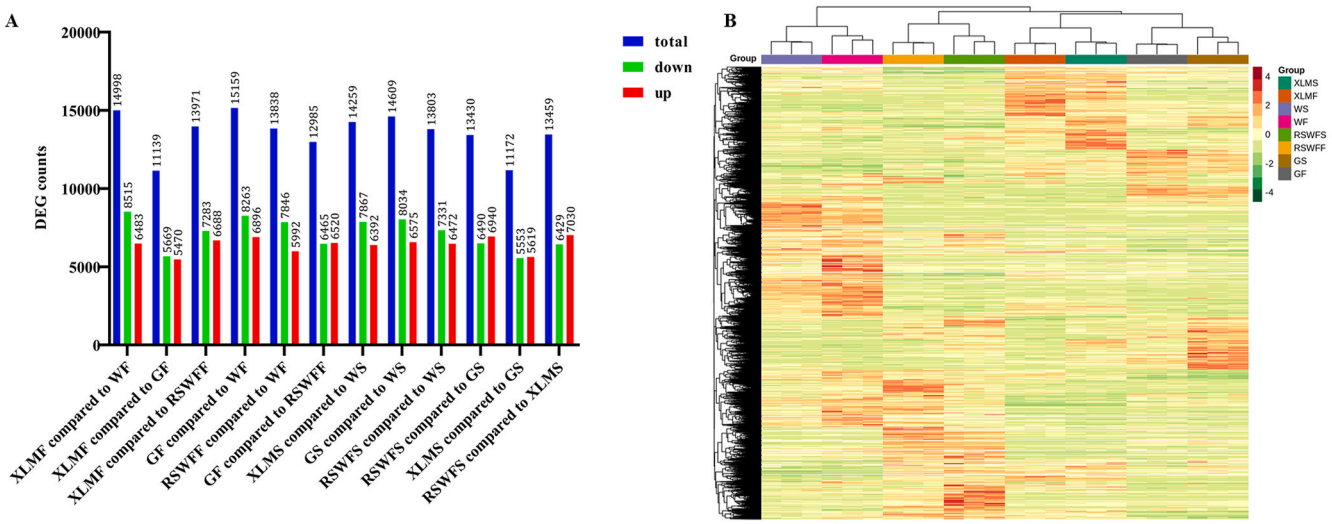


**Fig. 3.** Differentially expressed genes (DEGs) in the flesh and skin of different radish varieties. (A) Number of upregulated and downregulated DEGs in each comparison. (B) Heat map of HCA of the DEGs. Each DEG is represented by a row, and each sample is represented by a column. Red indicates high expression levels, and green indicates relatively low expression levels.

XLMF compared to WF, XLMF compared to GF, XLMF compared to RSWFF, GF compared to WF, RSWFF compared to WF, and GF compared to RSWFF, respectively. As for radish skin, there were 14259, 14609, 13803, 13430, 11172, and 13459 DEGs for XLMS compared to WS, GS compared to WS, RSWFS compared to WS, RSWFS compared to GS, XLMS compared to GS, and RSWFS compared to XLMS, respectively. Furthermore, HCA of the obtained DEGs was conducted and a heat map was constructed (Fig. 3B). The heat map reflected directly that each group had a distinct transcript profile. These DEGs may be potential regulators of differences in quality characteristics among different radish varieties.

To validate the transcriptome data, 12 DEGs, including 6 genes

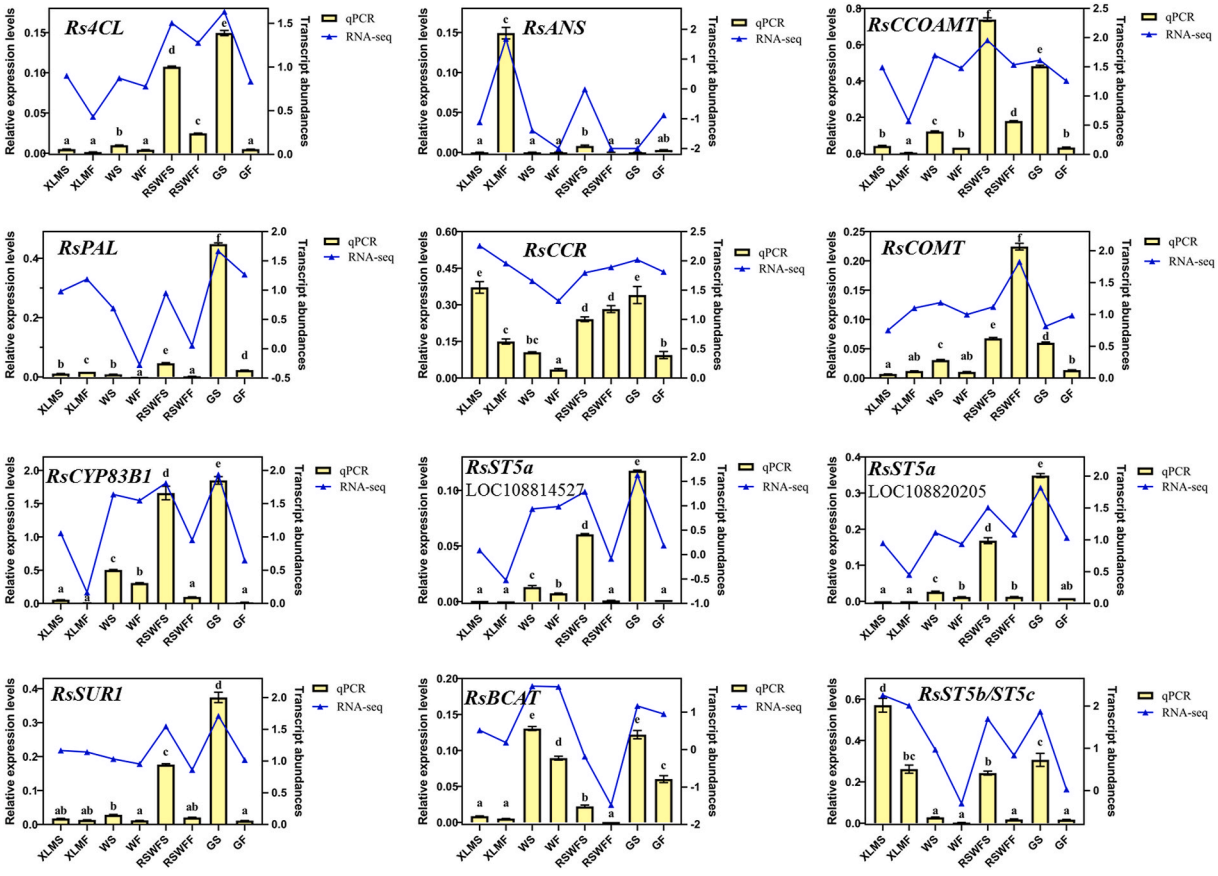


**Fig. 4.** Validation of the transcriptome data using RT-qPCR. The blue lines represent the RNA-seq data expressed in log-transformed FPKM (right y-axis), and the yellow bars indicate the RT-qPCR data measured by the delta CT method (left y-axis). Values without a common letter within the same gene were significantly different, $p < 0.05$. The significant differences among different groups were analyzed by LSD test.

involved in GSL biosynthesis and 6 genes related to flavonoid biosynthesis and phenylpropanoid biosynthesis, were randomly selected to assess their expression profiles in four radish varieties using RT-qPCR (Fig. 4). The results showed that *RsCYP83B1* (LOC108829823), *RsSUR1* (LOC108813271), and *RsST5a* (LOC108814527, LOC108820205) were more highly expressed in GS ($p < 0.05$). *RsST5b/ST5c* (LOC108823890) expression level was the highest in XLMS ($p < 0.05$), followed by GS. The expression level of *RsBCAT* (LOC108838735) was relatively high in GS and WS ($p < 0.05$). Additionally, as for the genes in flavonoid biosynthesis and phenylpropanoid biosynthesis, *RsPAL* (LOC108812387) and *Rs4CL* (LOC108862381) were also significantly upregulated in GS ($p < 0.05$). The expression level of *RsANS* (LOC108843686) was significantly increased in XLMF ($p < 0.05$). The expression level of *RsCCOAMT* (LOC108819091) was the highest in RSWFS ($p < 0.05$). The expression level of *RsCOMT* (LOC108857322) was significantly increased in RSWFF ($p < 0.05$). *RsCCR* (LOC108843713) expression level was relatively higher in GS and XLMS ($p < 0.05$). All of these RT-qPCR results were consistent with the transcriptome analysis, indicating the reliability of the gene expression profiles detected by RNA-seq.

### 3.4. Integrative analysis between metabolomics and transcriptomics related to flavonoid biosynthesis in different radish varieties

To further understand the molecular basis and discover detailed information about the metabolic pathways in the taproots of different radish varieties, both the DEGs and metabolites were mapped to the KEGG database, and the metabolic pathways associated with flavonoid biosynthesis and accumulation, including flavonoid biosynthesis (map00941), flavone and flavonol biosynthesis (map00944), and phenylpropanoid biosynthesis (map00940), were constructed (Fig. 5). The expression profiles of the DEGs and metabolites mapped in these metabolic pathways in different radish varieties are also displayed in Fig. 5. The expression patterns of the transcription factors (TFs) involved in the regulation of flavonoids in different radish varieties are shown in Fig. S9. Altogether 19 genes (*RsCHS*, *RsCHI*, *RsF3H*, *RsDFR*, *RsANS*, *RsCYP75B1*, *RsFLS*, *RsPGT1*, *RsPAL*, *RsC4H*, *Rs4CL*, *RsHCT*, *RsC3′H*, *RsCCOAMT*, *RsCAD*, *RsCCR*, *RsCOMT*, *RsF5H*, and *RsBRT1*) were involved in these pathways related to flavonoid biosynthesis (Fig. 5). Among the 19 genes, the expression levels of *RsCHS* and *RsCCOAMT* were significantly increased in RSWFS ($p < 0.05$); the expression levels of *RsF3H*, *RsFLS*, *RsCYP75B1*, and *RsDFR* were the highest in XLMF ($p < 0.05$), followed by RSWFS; and the expression of *RsC4H* was significantly enhanced in GS ($p < 0.05$). Additionally, six *RsPAL* genes identified displayed different expression patterns. Similarly, five *Rs4CL*, seven *RsCHI*, and two *RsANS* genes with differential expression patterns were also identified. The above 19 genes performed crucial roles in flavonoid biosynthesis in the taproots of different radish varieties, which were considered key genes affecting the differential accumulation of flavonoids among different radish cultivars.

To gain insight into the regulatory network of the differential distribution of flavonoid-related metabolites among different radish varieties, the correlation analysis between the transcripts and metabolites related to flavonoid biosynthesis was carried out, and a co-expression network was established. As shown in Fig. 6, 22 metabolites relevant to flavonoid biosynthesis were significantly correlated with 153 DEGs including 136 structural genes and 17 TFs (Pearson correlation coefficient $R \geq 0.8$, $p < 0.05$) (Supplementary Tables S4 and S5). The 22 metabolites and 153 DEGs associated with flavonoid biosynthesis were grouped into five clusters (A-E). In cluster A, 1-O-sinapoyl-β-D-glucose

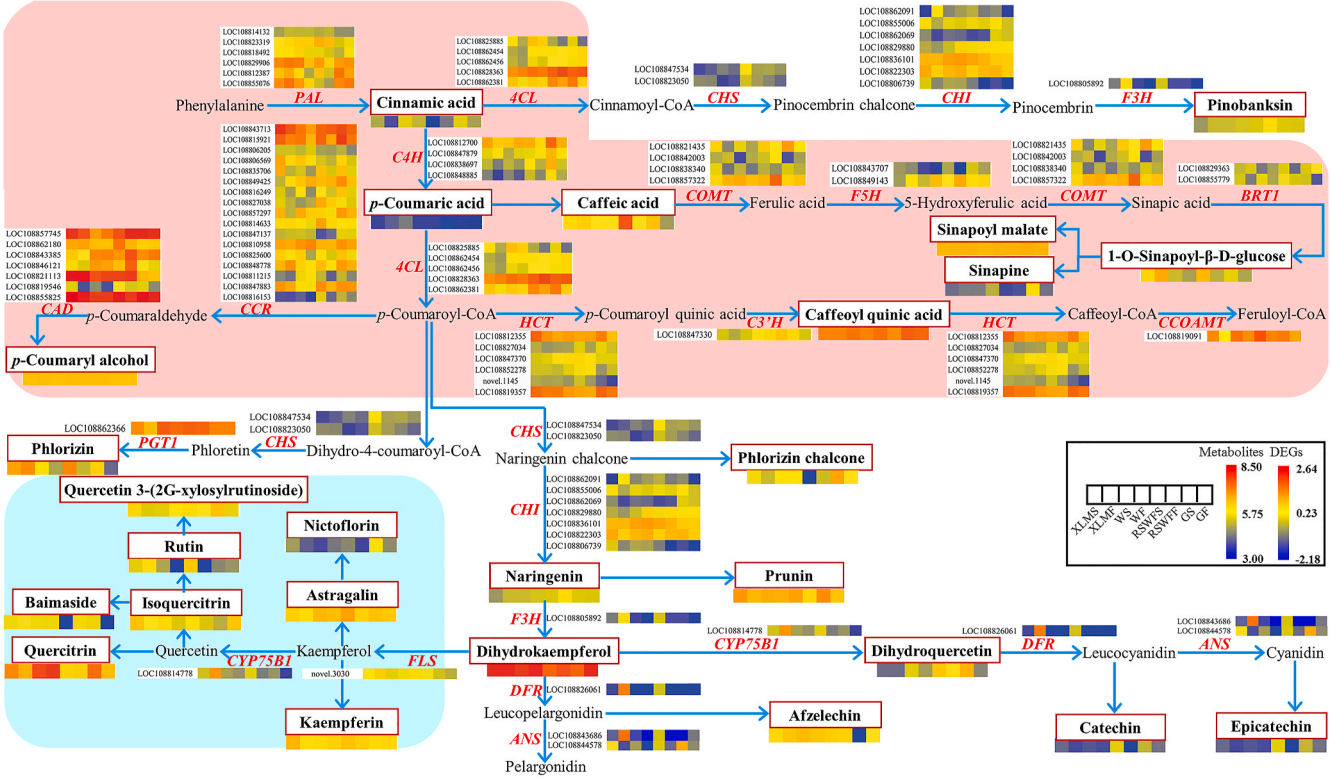


**Fig. 5.** Metabolic pathways associated with flavonoid biosynthesis and expression profiles of the related DEGs and metabolites in different radish varieties. These pathways are constructed based on the KEGG pathway. The pink box represents phenylpropanoid biosynthesis, the blue box represents flavone and flavonol biosynthesis, and the others belong to flavonoid biosynthesis. The right and left color scales from blue (low) to red (high) represent the log-transformed FPKM values of DEGs and the relative contents of metabolites, respectively. Heat maps are ordered by XLMS, XLMF, WS, WF, RSWFS, RSWFF, GS, and GF from left to right. Metabolites in red boxes indicate the identified metabolites mapped in phenylpropanoid biosynthesis (map00940), flavonoid biosynthesis (map00941), and flavone and flavonol biosynthesis (map00944).

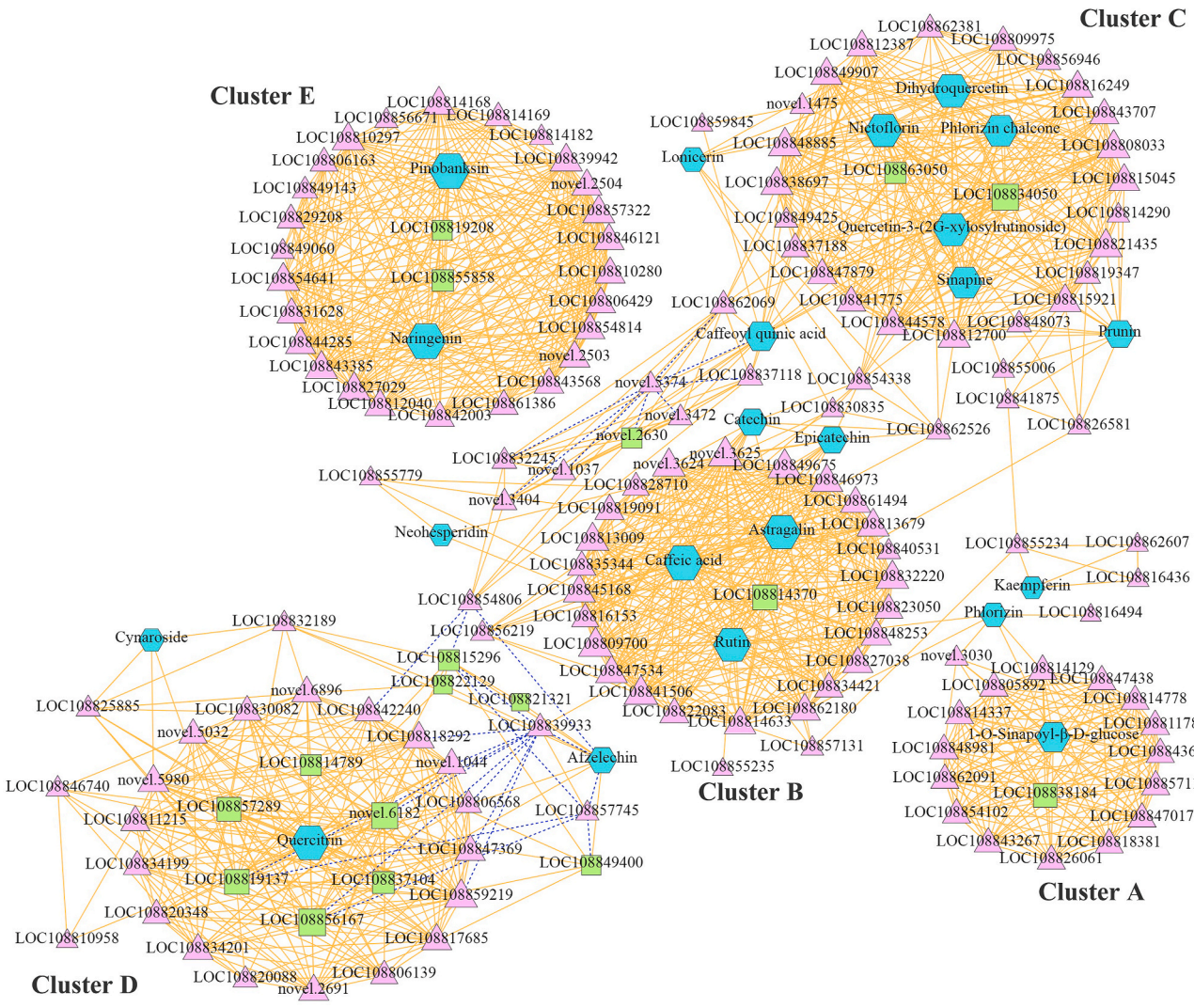


**Fig. 6.** Co-expression network between DEGs and metabolites relevant to flavonoid biosynthesis. Correlation relationships with Pearson correlation coefficient R ≥ 0.8 are shown. Cyan hexagons represent metabolites; pink triangles represent structural genes; and green squares represent TFs. Node size reflects its connectivity to other DEGs/metabolites. Orange solid lines represent positive correlations, and blue dashed lines represent negative correlations.

was significantly increased in XLMF ($p < 0.05$), and was highly correlated with 16 genes including *RsANS*, *RsCHS*, *RsFLS*, *RsF3H*, *RsCHI*, *RsCYP75B1*, *RsDFR*, and *RsIF7MAT* as well as transcription factor *RsTT8*. Three metabolites in cluster B, including rutin, astragalin, and caffeic acid, were more elevated in RSWFS ($p < 0.05$). A total of 21 genes, 21 genes, and 23 genes were found to be highly correlated with rutin, astragalin, and caffeic acid, respectively. These three metabolites were also highly correlated with transcription factor *RsTCP15*. Remarkably, the contents of epicatechin and catechin were also the highest in RSWFS ($p < 0.05$). In cluster C, five metabolites including dihydroquercetin, quercetin-3-(2G-xylosylrutinoside), nictoflorin, phlorizin chalcone, and sinapine were significantly increased in GS ($p < 0.05$). A total of 18 genes, 19 genes, 17 genes, 15 genes, and 15 genes were found to be highly correlated with quercetin-3-(2G-xylosylrutinoside), dihydroquercetin, nictoflorin, phlorizin chalcone, and sinapine, respectively. In cluster D, quercitrin was significantly increased in WF and WS ($p < 0.05$), and was highly correlated with 21 genes such as *RsHCT*, *RsCCR*, and *RsCCOAMT*. Two metabolites in cluster E, including pinobanksin and naringenin, were significantly elevated in RSWFF ($p < 0.05$), and were highly correlated with 26 genes such as *RsCOMT*, *RsF5H*, *RsCAD*, and *RsCCOAMT*. Overall, these results indicated that the synergistic expression and possible interaction of the above differential genes and TFs contributed to the various accumulation patterns of flavonoids among different radish varieties.

### 3.5. Integrative analysis between metabolomics and transcriptomics related to GSL biosynthesis in different radish varieties

To decipher the underlying mechanisms responsible for the differential accumulation of GSLs among different radish varieties, GSL biosynthesis pathway in the taproots of four radish varieties was constructed based on KEGG database (map00966), as shown in Fig. 7. The expression profiles of the DEGs and metabolites mapped in this metabolic pathway in different radish varieties are also displayed in Fig. 7. The expression patterns of the TFs involved in the regulation of GSLs in different radish varieties are shown in Fig. S10. A total of ten genes (*RsBCAT3*, *RsSUR1*, *RsUGT74B1*, *RsST5a*, *RsST5b/ST5c*, *RsCYP83B1*, *RsCYP79B2*, *RsCYP79B3*, *RsIPMI-LSU1*, *RsIPMI-SSU2*) and six differential metabolites (3-(methylthio)propyl GSL, 4-methylthiobutyl GSL, benzyl GSL, 3-indolylmethyl GSL, 5-methylthiopentyl GSL, 7-methylthioheptyl GSL) were involved in GSL biosynthesis pathway (Fig. 7). Among the six GSLs, the content of 3-(methylthio)propyl GSL was the highest in RSWFS ($p < 0.05$). 4-Methylthiobutyl GSL was significantly increased in GS and GF ($p < 0.05$). 5-Methylthiopentyl GSL was significantly elevated in the skin, but obviously low in the flesh, of all radish varieties ($p < 0.05$). 7-Methylthioheptyl GSL and benzyl GSL were the

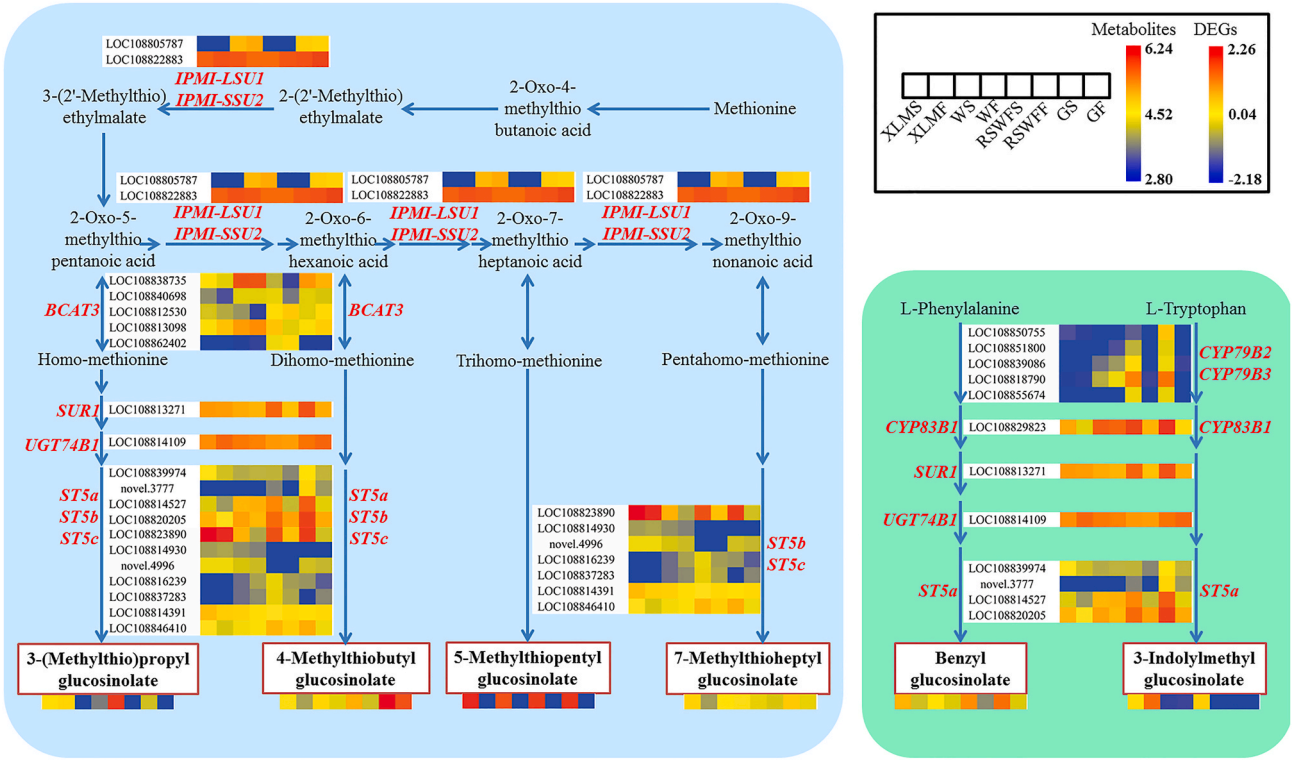


**Fig. 7.** Glucosinolate biosynthesis pathway and expression profiles of the related DEGs and metabolites in different radish varieties. This pathway is constructed based on the KEGG pathway. The right and left color scales from blue (low) to red (high) represent the log-transformed FPKM values of DEGs and the relative contents of metabolites, respectively. Heat maps are ordered by XLMS, XLMF, WS, WF, RSWFS, RSWFF, GS, and GF from left to right. Metabolites in red boxes indicate the identified metabolites mapped in glucosinolate biosynthesis pathway (map00966). The blue box represents the glucosinolate biosynthesis pathway from methionine. The green box represents the glucosinolate biosynthesis pathway from L-phenylalanine and L-tryptophan.

most abundant in GS ($p < 0.05$). The concentration of 3-indolylmethyl GSL was the highest in XLMF ($p < 0.05$). In brief, the six GSLs were specifically different depending on the radish varieties and there were distinct differences between radish skin and flesh. Also, the above ten genes could be considered key genes affecting the differential accumulation of GSLs among different radish varieties.

A co-expression network of the DEGs and metabolites related to GSL biosynthesis was established (Fig. 8). Four metabolites, including benzyl GSL, 4-methylthiobutyl GSL, 3-(methylthio)propyl GSL, and 5-methylthiopentyl GSL, were significantly correlated with 17 DEGs including 11 structural genes and 6 TFs, with Pearson correlation coefficient R ≥ 0.8 ($p < 0.05$) (Supplementary Tables S6 and S7). Among the four metabolites, benzyl GSL was found to be significantly positively correlated with *RsCYP83B1* (LOC108829823), *RsSUR1* (LOC108813271), *RsST5a* (LOC108814527, LOC108820205), *RsST5b/ST5c* (LOC108846410), *RsCYP79B2* (LOC108818790, LOC108855674), and *RsCYP79B3* (LOC108850755, LOC108851800), as well as transcription factor *RsMYB34* (LOC108829872), indicating that the accumulation of benzyl GSL in radish taproots is strongly influenced by the co-expression of these genes and the TF *RsMYB34*. 4-Methylthiobutyl GSL was found to be significantly positively correlated with *RsST5a* (LOC108814527, LOC108820205, novel. 3777) and *RsCYP79B3* (LOC108850755, LOC108851800), as well as 3 TFs including *RsMYB34* (LOC108829872). Among these correlations, the correlation coefficient of benzyl GSL and *RsSUR1* (LOC108813271) was highest (R = 0.98, $p = 6.70 \times 10^{-16}$), which suggests that *RsSUR1* may play an important role in the biosynthesis of benzyl GSL in radish.

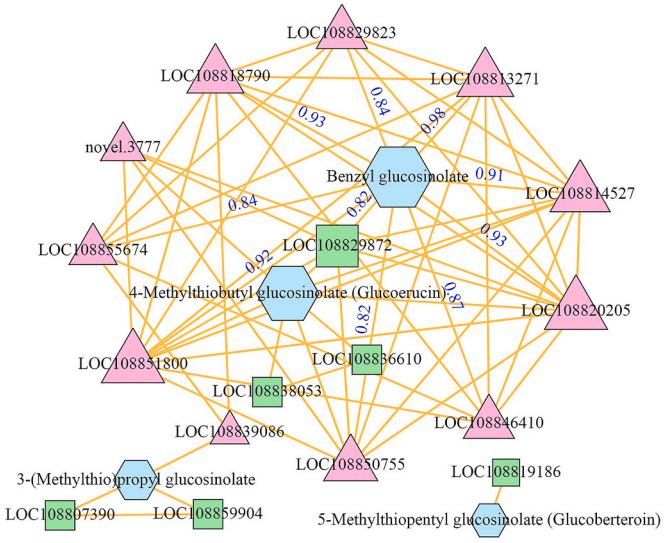


**Fig. 8.** Co-expression network between DEGs and metabolites relevant to glucosinolate biosynthesis. Correlation relationships with Pearson correlation coefficient R ≥ 0.8 are shown. Blue hexagons represent metabolites; pink triangles represent structural genes; and green squares represent TFs. Node size reflects its connectivity to other DEGs/metabolites. Orange solid lines represent positive correlations. The correlation coefficients of benzyl glucosinolate and 10 DEGs are marked with blue.

## 4. Discussion

As one of the most important commercial vegetable crops worldwide, radish plays critical roles in human diet and health. The previous studies have investigated specific categories of metabolites, such as anthocyanins and GSLs, concerning their biosynthesis pathways and regulatory mechanisms (Zhang et al., 2021; Liu et al., 2019; Muleke

et al., 2017; Li et al., 2022; Kang et al., 2020; Gao et al., 2019; Sun et al., 2018; Park et al., 2011). However, the overall differences in secondary metabolite profiles of different tissues among different radish varieties have not yet been clear until now. Moreover, the molecular regulatory mechanisms responsible for the differential accumulation of flavonoids and GSLs in different tissues of different radish varieties remain to be less-thoroughly understood. Here, through the comprehensive and comparative analysis of secondary metabolite profiles and transcriptome, we found that the flesh and skin of different radish cultivars had distinct metabolic profiles and gene expression patterns. Moreover, we also discovered key metabolic pathways responsible for the diversities of quality among different varieties, and identified key genes regulating the differential accumulation of flavonoids and GSLs among different radish varieties. Further, systematical biosynthetic pathways of flavonoids and GSLs and co-expression networks between genes and metabolites were constructed, thus achieving initial goal of this study and expanding our understanding of the accumulation patterns and regulatory mechanisms of bioactive components in different radish cultivars.

Altogether 352 secondary metabolites were identified in radish in this study, including 118 flavonoids and 95 phenolic acids, both of which accounted for 60.51% of the identified compounds, indicating that flavonoids and phenolic acids in radish were dominant bioactive constituents. Flavonoids are important plant pigments (Hostetler et al., 2017). It has been reported that flavonoids, as pivotal ingredients of the human diet, have wide health benefits, such as antioxidation, anti-inflammation, cardioprotection, antihypertension, anticarcinogenic activity, and blood glucose regulation (Rathod et al., 2023). In the present study, we discovered that the total flavonoids were highest in red-colored radish tissue XLMF and RSWFS ($p < 0.05$). Their antioxidant capacity, meanwhile, was also highest ($p < 0.05$). Additionally, the different tissues of different radish varieties revealed distinct flavonoid accumulation profiles, which was consistent with the observations of Zhang et al. who found different profiles of flavonoids among different colored radishes (Zhang et al., 2020a). Specifically, we found that rutin, astragalin, caffeic acid, epicatechin and catechin were significantly increased in RSWFS ($p < 0.05$), with a similar trend with the previous studies which showed that caffeic acid and epicatechin were higher in the skin of Hong Feng No.1 radish ($p < 0.05$) (Park et al., 2011), epicatechin was abundant in MSH radish with red skin and white flesh (Mei et al., 2022), and the level of catechin was upregulated in the red and purple radishes (Zhang et al., 2021). Catechin and epicatechin have been recognized to possess numerous pharmacological activities, such as antioxidative, anticancer, anti-aging, and immunomodulatory properties (Meyer et al., 1998; Ebeler et al., 2002). Besides, it is worth noting that cyanidin-3-O-(6″-O-feruloyl)sophoroside-5-O-glucoside, a kind of anthocyanin responsible for color pigmentation, was significantly increased in RSWFS ($p < 0.05$), which was similar to the findings of Zhang et al. who found that red radish was enriched with cyanidin (Zhang et al., 2020a). Hence, RSWFS is a richer source of rutin, astragalin, caffeic acid, epicatechin, catechin, and anthocyanin, with health-promoting value. Additionally, our results revealed that pinobanksin and naringenin were significantly elevated in RSWFF ($p < 0.05$). Pinobanksin has been reported to have antioxidative, antimicrobial, antiproliferative, and antiangiogenic activities (Zheng et al., 2018; Bang and Ahn, 2021). Naringenin has been shown to possess anticancer, anti-inflammatory, antioxidative, and anti-diabetic activities (Joshi et al., 2018). Thus, RSWFF is a better source of pinobanksin and naringenin, beneficial to human health. Also, we discovered that 1-O-sinapoyl-β-D-glucose was significantly increased in XLMF ($p < 0.05$); dihydroquercetin, quercetin-3-(2G-xylosylrutinoside), nictoflorin, phlorizin chalcone, and sinapine were significantly increased in GS ($p < 0.05$); while quercitrin was more elevated in WF and WS ($p < 0.05$). These results reflected the unique flavonoid metabolic profiles in each radish cultivar, greatly contributing to the distinct differences in nutritional quality and coloration among different radish varieties.

The discrepancies in accumulation profiles of flavonoids in different tissues of different radish varieties are ascribable to differences in the unique expression patterns of the overall set of genes regulating flavonoid biosynthesis. In this study, *RsCHS*, *RsCHI*, *RsF3H*, *RsDFR*, *RsANS*, *RsCYP75B1*, *RsFLS*, *RsPGT1*, *RsPAL*, *RsC4H*, *Rs4CL*, *RsHCT*, *RsC3′H*, *RsCCOAMT*, *RsCAD*, *RsCCR*, *RsCOMT*, *RsF5H*, and *RsBRT1* were identified as key genes regulating flavonoid biosynthesis and accumulation in different radish varieties. Among these key genes, the expression of *RsCHS* was significantly increased in RSWFS ($p < 0.05$). Similarly, a previous study showed that *RsCHS* expression level was the highest in the skin of Hong Feng No.1 radish with red skin and white flesh ($p < 0.05$) (Park et al., 2011). Also, *RsCHS* was found upregulated in the HX-3 and WG-3 radishes with red skin and red flesh (Gao et al., 2019). Other work also showed that *RsCHS3* correlated positively with total anthocyanin in radish (Muleke et al., 2017). It is generally believed that CHS proteins have multiple functions, including pigment biosynthesis, defense against pathogens, protection from UV radiation, and pollen fertility (Deng et al., 2014). Additionally, we found that the expression levels of *RsF3H*, *RsFLS*, *RsCYP75B1*, *RsDFR*, and *RsANS* (LOC108843686) were the highest in XLMF ($p < 0.05$), followed by RSWFS. These results were in line with the findings of Zhang et al. and Sun et al., both of whom found that *RsFLS*, *RsCYP75B1*, *RsDFR*, and *RsANS* were significantly upregulated in the flesh of Xinlimei radish (Zhang et al., 2021), and that the expression levels of *F3H*, *DFR*, and *ANS* were higher in Xinlimei radish than those in white radish (Sun et al., 2018), respectively. Besides, we also discovered that the expression level of *RsCCOAMT* was significantly increased in RSWFS ($p < 0.05$), which was similar to the observations reported by Zhang et al. who found that *RsCCOAMT* was abundant in the red-color radishes but undetectable in white radishes (Zhang et al., 2021). In brief, the above genes including *RsCHS*, *RsCCOAMT*, *RsF3H*, *RsFLS*, *RsCYP75B1*, *RsDFR*, and *RsANS* were significantly upregulated in red-colored radish tissue RSWFS and XLMF, implying that these genes could contribute to the increase of total flavonoids, total polyphenols, and antioxidant capacity. Interestingly, our results also showed that six *RsPAL* genes identified displayed different expression patterns, implying divergent functions (Lai et al., 2015). Similarly, five *Rs4CL*, seven *RsCHI*, and two *RsANS* genes with differential expression patterns were also identified. Furthermore, through the correlation analysis between the metabolome and transcriptome, we found that 22 flavonoid-related metabolites were significantly correlated with 153 DEGs associated with flavonoid biosynthesis ($R \geq 0.8$, $p < 0.05$), which were grouped into five clusters (A-E), implying that the genes in each cluster might be functionally connected to the flavonoids in the corresponding cluster, regulating the biosynthesis and accumulation of flavonoids in different radish varieties. The co-expression network analysis between metabolomics and transcriptomics has been rarely reported in previous studies, and only Zhang et al. constructed a connection network between genes and flavonoids thus far (Zhang et al., 2021). Our results also indicate that a single gene is not responsible for flavonoid accumulation and that flavonoid biosynthesis involves the coordinated mechanism of numerous genes.

GSLs are also important and unique bioactive components in radish. It was reported that GSLs and their degradation products isothiocyanates are beneficial to human health because of their biological activities, such as anticarcinogenic activity, anti-inflammation, and cardiovascular protection (Curtis, 2003; Soundararajan and Kim, 2018), strongly influencing the nutritional quality as well as pungent taste of radish (Holst and Williamson, 2004; Curtis, 2003). Li and Kang et al. detected six and ten GSLs in radish, respectively (Li et al., 2022; Kang et al., 2020). In this study, we identified 28 GSLs, of which six GSL components were involved in GSL biosynthesis pathway. Among the six GSLs, 4-methylthiobutyl GSL was significantly increased in GS and GF ($p < 0.05$). We also found that 7-methylthioheptyl GSL, benzyl GSL, 6-(methylsulfinyl)hexyl GSL, 7-(methylsulfinyl) heptyl GSL, 4-hydroxyindol-3-ylmethyl GSL, and 8-methylsulfinyl-3-oxooctyl GSL were the most abundant in GS ($p < 0.05$). These results were similar to the

findings of Mei et al. who found that 6-(methylsulfinyl)hexyl GSL, 7-(methylsulfinyl) heptyl GSL, and 4-hydroxyindol-3-ylmethyl GSL were more abundant in SDQ radish with green flesh and green skin than the other samples (Mei et al., 2022). Additionally, our results showed that 4-methylthio-3-butenyl GSL was significantly increased in RSWFS ($p < 0.05$). It has been reported that 4-methylthio-3-butenyl GSL is the predominant GSL in radish (Yi et al., 2016). Besides, we also discovered that the concentration of 3-indolylmethyl GSL was the highest in XLMF ($p < 0.05$). Yet, a previous study showed that 3-indolylmethyl GSL was most abundant in SDQ radish, but Xinlimei radish was not included in that study (Mei et al., 2022). Thus, it can be concluded that the unique accumulation patterns of GSLs in each radish varieties, to a large extent, contribute to the distinct differences in pungent taste and nutritional quality among different radish cultivars.

Better understanding of the key genes and molecular mechanism regulating GSLs accumulation provides a blueprint for genetic improvement of quality traits in radish molecular breeding research to increase the accumulation of beneficial GSLs for enhancing the health benefits and commercial value of radish. Previous research has confirmed that *BCAT3*, *IPMI-LSU1*, *IPMI-SSU2*, *CYP83B1*, *SUR1*, *UGT74B1*, *ST5a*, and *ST5b/ST5c* genes are known to be the major genes involved in GSL biosynthesis (Liu et al., 2014). In this study, we identified 10 key genes regulating GSL biosynthesis and accumulation in different radish cultivars. Among these key genes, the expression levels of *RsCYP83B1*, *RsSUR1*, and *RsST5a* were the highest in GS ($p < 0.05$). *RsST5b/ST5c* expression level was the highest in XLMS ($p < 0.05$), followed by GS. A previous study showed that the expression levels of *RsSUR1* and *RsST5b* were significantly higher in the radish genotypes with high GSL content, compared with a genotype with low content (Li et al., 2022). Besides, other work showed that the expression levels of *IPMI-LSU1*, *IPMI-SSU2*, *SUR1*, *UGT74B1*, and *ST5b/ST5c* were significantly higher, while *CYP79B2*, *CYP79B3*, *CYP83B1*, and *ST5a* were at low levels of expression, in the radish with high GSL content (Kang et al., 2020). The differences among the different studies could be attributed to the discrepancies in the genetic background and growing conditions of radish accessions used in different researches. However, as to the different tissues of different radish varieties, the accumulation patterns and regulatory mechanisms of GSLs have rarely been reported to our knowledge. Additionally, through the integrative analysis between the metabolome and transcriptome, we found that benzyl GSL, 4-methylthiobutyl GSL, 3-(methylthio)propyl GSL, and 5-methylthiopentyl GSL were significantly correlated with 11 structural genes including *RsCYP83B1*, *RsSUR1*, *RsST5a*, *RsST5b/ST5c*, *RsCYP79B2*, and *RsCYP79B3*, as well as 6 TFs such as *RsMYB34*. In order to confirm and apply our results, further studies are needed, such as transgenic function verification of key genes, for radish genome design breeding research to produce more beneficial phytochemicals for promoting human health in the future.

## 5. Conclusions

This study provides a global view of the secondary metabolite profiles and gene expression patterns of four popular radish varieties, and further reveals the regulatory mechanisms of the differential accumulation of flavonoids and GSLs in different tissues among different radish cultivars. The accumulation profiles of secondary metabolites in the flesh and skin of different radish varieties were notably distinct. The differential metabolites were mostly enriched in flavonoid biosynthesis, flavone and flavonol biosynthesis, phenylpropanoid biosynthesis, and GSL biosynthesis pathway, greatly contributing to the diversities of coloration, flavor, taste, and nutritional quality among different cultivars. Furthermore, 19 key genes regulating the differential accumulation of flavonoids among different radish varieties were identified. Among them, *RsCHS*, *RsCCOAMT*, *RsF3H*, *RsFLS*, *RsCYP75B1*, *RsDFR*, and *RsANS* were significantly upregulated in red-colored radish tissue RSWFS and/or XLMF, implying that these genes could contribute to the increase of total flavonoids, total polyphenols, and antioxidant capacity. Also, 10 key genes affecting the differential accumulation of GSLs among different radish cultivars were identified, such as *RsCYP83B1*, *RsSUR1*, and *RsST5a* that were significantly increased in GS. Further, systematical biosynthetic pathways of flavonoids and GSLs and co-expression networks between genes and metabolites were constructed, reflecting the synergistic expression and coordinated mechanism of the DEGs regulating the differential accumulation patterns of flavonoids and GSLs among different radish varieties. Overall, this study comprehensively characterizes secondary metabolites in different radish cultivars at the metabolic and molecular levels and provides a novel insight into the biosynthesis and accumulation of flavonoids and GSLs in different radish varieties through the integrative analysis between metabolomics and transcriptomics. These findings provide better understanding about the mechanisms of radish quality formation, thereby providing a molecular basis for breeding and cultivation of radish with excellent nutritional quality.

## CRediT authorship contribution statement

**Da Cai:** Conceptualization, Investigation, Methodology, Formal analysis, Data curation, Writing – original draft, Writing – review & editing. **Yanjie Dong:** Validation, Visualization. **Lei Wang:** Resources. **Shancang Zhao:** Conceptualization, Supervision, Project administration, Funding acquisition, All authors have read and approved the final manuscript.

## Declaration of competing interest

The authors declare the following financial interests/personal relationships which may be considered as potential competing interests: Shancang Zhao reports financial support was provided by Shandong Provincial Science and Technology Agency. If there are other authors, they declare that they have no known competing financial interests or personal relationships that could have appeared to influence the work reported in this paper.

## Acknowledgements

Thanks for the support of the Shandong Provincial Natural Science Foundation (No. ZR2019PC022), the Agricultural Scientific and Technological Innovation Project of the Shandong Academy of Agricultural Sciences (No. CXGC2021A24), the Shandong Key R & D Plan (2019JZZY020903), and the Shandong Key R & D Plan (2023TZXD036).

## Appendix A. Supplementary data

Supplementary data to this article can be found online at https://doi.org/10.1016/j.crfs.2024.100938.

## Data availability

Data will be made available on request.

## References

Agricultural Industry Standard of China NY/T 1295-2007, 2007. Determination of flavones in buckwheat and its products.
Bang, H.-J., Ahn, M.-R., 2021. Antiangiogenic effect of pinobanksin on human umbilical vein endothelial cells. J. Funct.Foods 79, 104408.
Barillari, J., Cervellati, R., Paolini, M., Tatibouet, A., Rollin, P., Iori, R., 2005. Isolation of 4-methylthio-3-butenyl glucosinolate from Raphanus sativus sprouts (kaiware daikon) and its redox properties. J. Agric. Food Chem. 53, 9890–9896.
Bohm, B.A., 1998. Introduction to Flavonoids. Harwood academic publishers.
Curtis, I.S., 2003. The noble radish: past, present and future. Trends Plant Sci. 8, 305–307.
Deng, X., Bashandy, H., Ainasoja, M., Kontturi, J., Pietiainen, M., Laitinen, R.A., Albert, V.A., Valkonen, J.P.T., Elomaa, P., Teeri, T.H., 2014. Functional

diversification of duplicated chalcone synthase genes in anthocyanin biosynthesis of Gerbera hybrida. New Phytol. 201 (4), 1469–1483.
Ebeler, S.E., Brenneman, C.A., Kim, G.S., Jewell, W.T., Webb, M.R., Chacon-Rodriguez, L., MacDonald, E.A., Cramer, A.C., Levi, A., Ebeler, J.D., Islas-Trejo, A., Kraus, A., Hinrichs, S.H., Clifford, A.J., 2002. Dietary catechin delays tumor onset in a transgenic mouse model. Am. J. Clin. Nutr. 76 (4), 865–872.
Gao, J., Li, W.-B., Liu, H.-F., Chen, F.-B., 2019. De novo transcriptome sequencing of radish (Raphanus sativus L.) fleshy roots: analysis of major genes involved in the anthocyanin synthesis pathway. BMC Mol. Cell Biol. 20, 45.
Halkier, B.A., Gershenzon, J., 2006. Biology and biochemistry of glucosinolates. Annu. Rev. Plant Biol. 57, 303–333.
Heng, Z., Xu, X., Xu, X., Li, Y., Wang, H., Huang, W., Yan, S., Li, T., 2023. Integrated transcriptomic and metabolomic analysis of chili pepper fruits provides new insight into the regulation of the branched chain esters and capsaicin biosynthesis. Food Res. Int. 169, 112856.
Holst, B., Williamson, G., 2004. A critical review of the bioavailability of glucosinolates and related compounds. Nat. Prod. Rep. 21 (3), 425–447.
Holton, T.A., Cornish, E.C., 1995. Genetics and biochemistry of anthocyanin biosynthesis. Plant Cell 7, 1071–1083.
Hostetler, G.L., Ralston, R.A., Schwartz, S.J., 2017. Flavones: food sources, bioavailability, metabolism, and bioactivity. Adv. Nutr. 8, 423–435.
Jing, P., Zhao, S.J., Ruan, S.Y., Xie, Z.H., Dong, Y., Yu, L.L., 2012. Anthocyanin and glucosinolate occurrences in the roots of Chinese red radish (Raphanus sativus L.), and their stability to heat and pH. Food Chem. 133, 1569–1576.
Joshi, R., Kulkarni, Y.A., Wairkar, S., 2018. Pharmacokinetic, pharmacodynamic and formulations aspects of Naringenin: an update. Life Sci. 215, 43–56.
Kang, J.N., Won, S.Y., Seo, M.S., Lee, J., Lee, S.M., Kwon, S.J., Kim, J.S., 2020. Induction of glucoraphasatin biosynthesis genes by MYB29 in radish (Raphanus sativus L.) roots. Int. J. Mol. Sci. 21, 5721.
Kim, D., Langmead, B., Salzberg, S.L., 2015. HISAT: a fast spliced aligner with low memory requirements. Nat. Methods 12, 357–360.
Lai, B., Hu, B., Qin, Y.-H., Zhao, J.-T., Wang, H.-C., Hu, G.-B., 2015. Transcriptomic analysis of Litchi chinensis pericarp during maturation with a focus on chlorophyll degradation and flavonoid biosynthesis. BMC Genom. 16, 225.
Li, S., Deng, B., Tian, S., Guo, M., Liu, H., Zhao, X., 2021. Metabolic and transcriptomic analyses reveal different metabolite biosynthesis profiles between leaf buds and mature leaves in Ziziphus jujuba mill. Food Chem. 347, 129005.
Li, X., Wang, P., Wang, J., Wang, H., Liu, T., Zhang, X., Song, J., Yang, W., Wu, C., Yang, H., Liu, L., Li, X., 2022. A comparative transcriptome and metabolome combined analysis reveals the key genes and their regulatory model responsible for glucoraphasatin accumulation in radish fleshy taproots. Int. J. Mol. Sci. 23, 2953.
Liu, S., Liu, Y., Yang, X., Tong, C., Edwards, D., Parkin, I.A., Zhao, M., Ma, J., Yu, J., Huang, S., et al., 2014. The Brassica oleracea genome reveals the asymmetrical evolution of polyploid genomes. Nat. Commun. 5, 3930.
Liu, T., Zhang, Y., Zhang, X., Sun, Y., Wang, H., Song, J., Li, X., 2019. Transcriptome analyses reveal key genes involved in skin color changes of 'Xinlimei' radish taproot. Plant Physiol. Biochem. 139, 528–539.
Mei, S., He, Z., Zhang, J., 2022. Identification and analysis of major flavor compounds in radish taproots by widely targeted metabolomics. Front. Nutr. 9, 889407.
Meyer, A.S., Heinonen, M., Frankel, E.N., 1998. Antioxidant interactions of catechin, cyanidin, caffeic acid, quercetin, and ellagic acid on human LDL oxidation. Food Chem. 61, 71–75.
Muleke, E.M., Fan, L., Wang, Y., Xu, L., Zhu, X., Zhang, W., Cao, Y., Karanja, B.K., Liu, L., 2017. Coordinated regulation of anthocyanin biosynthesis genes confers varied phenotypic and spatial-temporal anthocyanin accumulation in radish (Raphanus sativus L.). Front. Plant Sci. 8, 1243.
National Standards of China GB 5009.3-2016, 2016. In: National Standards for Food Safety Determination of Moisture Content in Foods.
National Standards of China GB/T 8313-2018, 2018. In: Determination of Total Polyphenols and Catechins in Tea.
Park, N.I., Xu, H., Li, X., Jang, I.H., Park, S., Ahn, G.H., Lim, Y.P., Kim, S.J., Park, S.U., 2011. Anthocyanin accumulation and expression of anthocyanin biosynthetic genes in radish (Raphanus sativus). J. Agric. Food Chem. 59, 6034–6039.
Rathod, N.B., Elabed, N., Punia, S., Ozogul, F., Kim, S.-K., Rocha, J.M., 2023. Recent developments in polyphenol applications on human health: a review with current knowledge. Plants 12, 1217.
Razis, A.F.A., Bagatta, M., De Nicola, G.R., Iori, R., Ioannides, C., 2011. Up-regulation of cytochrome P450 and phase II enzyme systems in rat precision-cut rat lung slices by the intact glucosinolates, glucoraphanin and glucoerucin. Lung Cancer 71, 298–305.
Schmittgen, T.D., Livak, K.J., 2008. Analyzing real-time PCR data by the comparative $C_T$ method. Nat. Protoc. 3 (6), 1101–1108.
Soundararajan, P., Kim, J.S., 2018. Anti-carcinogenic glucosinolates in cruciferous vegetables and their antagonistic effects on prevention of cancers. Molecules 23, 2983.
Sun, Y., Wang, J., Qiu, Y., Liu, T., Song, J., Li, X., 2018. Identification of 'Xinlimei' radish candidate genes associated with anthocyanin biosynthesis based on a transcriptome analysis. Gene 657, 81–91.
Wang, F., Ji, G., Xu, Z., Feng, B., Zhou, Q., Fan, X., Wang, T., 2021. Metabolomics and transcriptomics provide insights into anthocyanin biosynthesis in the developing grains of purple wheat (Triticum aestivum L.). J. Agric. Food Chem. 69, 11171–11184.
Wang, S., Shen, S., Wang, C., Wang, X., Yang, C., Zhou, S., Zhang, R., Zhou, Q., Yu, H., Guo, H., et al., 2024. A metabolomics study in citrus provides insight into bioactive phenylpropanoid metabolism. Hortic. Res. 11, 267.
Yang, J., Chen, R., Wang, C., Li, C., Ye, W., Zhang, Z., Wang, S., 2024. A widely targeted metabolite modificomics strategy for modified metabolites identification in tomato. J. Integr. Plant Biol. 66, 810–823.
Yi, G., Lim, S., Chae, W.B., Park, J.E., Park, H.R., Lee, E.J., Huh, J.H., 2016. Root glucosinolate profiles for screening of radish (Raphanus sativus L.) genetic resources. J. Agric. Food Chem. 64, 61–70.
Zhang, X., Yue, Z., Mei, S., Qiu, Y., Yang, X., Chen, X., Cheng, F., Wu, Z., Sun, Y., Jing, Y., Liu, B., Shen, D., Wang, H., Cui, N., Duan, Y., Wu, J., Wang, J., Gan, C., Wang, J., Wang, X., Li, X., 2015. A de novo genome of a Chinese radish cultivar. Hortic. Plant J. 1, 155–164.
Zhang, J., Wang, H., Liu, Z., Liang, J., Wu, J., Cheng, F., Mei, S., Wang, X., 2018a. A naturally occurring variation in the BrMAM-3 gene is associated with aliphatic glucosinolate accumulation in Brassica rapa leaves. Hortic. Res. 5, 69.
Zhang, X., Su, N., Jia, L., Tian, J., Li, H., Huang, L., Shen, Z., Cui, J., 2018b. Transcriptome analysis of radish sprouts hypocotyls reveals the regulatory role of hydrogen-rich water in anthocyanin biosynthesis under UV-A. BMC Plant Biol. 18, 227.
Zhang, J., Qiu, X., Tan, Q., Xiao, Q., Mei, S., 2020a. A comparative metabolomics study of flavonoids in radish with different skin and flesh colors (Raphanus sativus L.). J. Agric. Food Chem. 68, 14463–14470.
Zhang, Q., Wang, L., Liu, Z., Zhao, Z., Zhao, J., Wang, Z., Zhou, G., Liu, P., Liu, M., 2020b. Transcriptome and metabolome profiling unveil the mechanisms of Ziziphus jujuba Mill. peel coloration. Food Chem. 312, 125903.
Zhang, J., Zhao, J., Tan, Q., Qiu, X., Mei, S., 2021. Comparative transcriptome analysis reveals key genes associated with pigmentation in radish (Raphanus sativus L.) skin and flesh. Sci. Rep. 11, 11434.
Zhang, J., Zhang, Z.-X., Wen, B.-Y., Jiang, Y.-J., He, X., Bai, R., Zhang, X.-L., Chai, W.-C., Xu, X.-Y., Xu, J., et al., 2023. Molecular regulatory network of anthocyanin accumulation in black radish skin as revealed by transcriptome and metabonome analysis. Int. J. Mol. Sci. 24, 13663.
Zheng, Y.Z., Deng, G., Chen, D.F., Liang, Q., Guo, R., Fu, Z.M., 2018. Theoretical studies on the antioxidant activity of pinobanksin and its ester derivatives: effects of the chain length and solvent. Food Chem. 240, 323–329.
Zhu, G., Wang, S., Huang, Z., Zhang, S., Liao, Q., Zhang, C., Lin, T., Qin, M., Peng, M., Yang, C., Cao, X., Han, X., Wang, X., van der Knaap, E., Zhang, Z., Cui, X., Klee, H., Fernie, A.R., Luo, J., Huang, S., 2018. Rewiring of the fruit metabolome in tomato breeding. Cell 172, 249–261.